A Torque Vectoring Strategy for Improving the Performance of a Rear Wheel Drive Electric Vehicle

Conference Paper · October 2015

DOI: 10.1109/VPPC.2015.7352887

CITATIONS
19

READS
3,790

3 authors:

Jyotishman Ghosh
Politecnico di Torino
7 PUBLICATIONS **61** CITATIONS
SEE PROFILE

Andrea Tonoli
Politecnico di Torino
194 PUBLICATIONS **1,761** CITATIONS
SEE PROFILE

N. Amati
Politecnico di Torino
138 PUBLICATIONS **1,069** CITATIONS
SEE PROFILE

A Torque Vectoring Strategy for Improving the Performance of a Rear Wheel Drive Electric Vehicle

Jyotishman Ghosh, Andrea Tonoli, Nicola Amati
Department of Mechanical and Aerospace Engineering
Politecnico di Torino
Turin, Italy
Email: jyotishman.ghosh@polito.it

***Abstract*—This article presents a feedback controller for the torque vectoring control of a rear wheel drive electric vehicle. The main objective of the work presented is to improve the vehicle maneuverability. Distribution of driving/braking torque between left and right wheels allows optimal usage of tire forces which leads to better handling behavior. The controller performance is evaluated by executing steady state and dynamic maneuvers on a multi-body vehicle model. The dynamic maneuvers include numerical simulations around a race track in order to understand the influence of torque vectoring across the complete working range of the tires. Results indicate that torque vectoring control is able to improve the performance of the vehicle in terms of its yaw response and racetrack lap times by better exploitation of the tire forces.**

I. Introduction

Direct yaw moment control (DYC) can be used to alter the lateral dynamics behavior of a vehicle. DYC involves the generation of a yaw moment by various actuators. A yaw moment can be used to control the lateral forces generated by the tires. This can result in generation of desired handling behavior in vehicles. Researchers have made use of this idea in the past to develop control strategies which result in desired vehicle response. Shibahata in [1] mentions that the limits of vehicle maneuverability can be enlarged by using DYC. Abe in [2] uses sliding surface controller to control the sideslip angle of the vehicle. Brakes are used to generate the desired yaw moment. The controller is able to improve vehicle stability in extreme maneuvers. A downside of using brakes to generate a yaw moment is that the vehicle slows down as the brakes are applied. A workaround this problem is to use torque vectoring (TV) which involves the transfer of driving/braking torque from the left to the right wheels or vice versa. Torque vectoring differentials allow torque to be distributed unevenly between the left and the right wheels which lead to the generation of a yaw moment. De Novellis et al. in [3] show that a desired understeer characteristic behavior can be achieved with such a TV differential. The controlled vehicle has higher cornering capabilities due to an increase in maximum possible lateral acceleration. In the domain of electric vehicles, it is possible to have TV without the need of a TV differential given that at least two wheels are driven independently by separate electric motors. Authors in [4], [5] have proposed control algorithms for such systems. Above methods are based on generating yaw moment such that a predefined understeering gradient is achieved. Once the vehicle states like the sideslip angle, yaw rate cross safety thresholds, the controller switches from a performance based controller to a stability controller and generates yaw moments to push the vehicle back to stability. These stability control systems are mostly map based and their algorithms mostly try to improve the performance by a certain level while keeping focus on stabilizing the vehicle in all scenarios. However, to be able to extract the best cornering performance, a study indicating how to maximize the handling limit of the vehicle is also required. Sawase in [6] assumes the shape of the friction ellipse to be circular and calculates the limit for vehicle handling. In most vehicles, the friction circle is slightly elliptical in shape [7]. Thus, a more detailed study about the interaction of lateral and longitudinal forces at limit conditions is also warranted.

This paper proposes a control logic for left right torque vectoring which allows maximization of the extractable lateral force from the tires by making them work in the optimal operating region. The objective of this work is to lower the understeering gradient of the vehicle, increase the maximum lateral acceleration and also increase the area under the a_x vs. a_y plot. The main contribution of this article is to include the effect of rear roll steer in the generation of an ideal torque vectoring moment. Another contribution is the study of the performance of a TV controller for improving race track lap times by analyzing the a_x vs. a_y plot generated by the active and passive vehicles.

The paper is organized as follows: Section II depicts the vehicle plant model used for the simulations. Section III first illustrates the principles of torque vectoring and then elaborates on the used control architecture. Section IV shows the simulation results followed by section V which presents the conclusions.

II. Vehicle Model

The performance of the TV controller is studied on a rear wheel drive electric vehicle which has been modeled in VI-CarRealTime (VI-Grade GmbH)-Simulink co-simulation environment. The chassis model includes the dynamics due to sprung and unsprung masses. Nonlinear multibody dynamics of the suspension and the steering system has been also

#Understeer and oversteer are vehicle dynamics terms used to describe the sensitivity of a vehicle to steering. Oversteer is what occurs when a car turns (steers) by more than the amount commanded by the driver. Conversely, understeer is what occurs when a car steers less than the amount commanded by the driver.

TABLE I
VEHICLE PARAMETERS

Property	Symbol	Value	Unit
mass	m	1150	kg
CG from front axle	a	1000	mm
CG from rear axle	b	1500	mm
CG height from ground	h_{cg}	415	mm
Track width	t	1750	mm
Yaw moment of inertia	I_{zz}	850	kgm^2
Maximum Torque of Electric motor	T_{max}	240	Nm
Maximum speed of Electric motor	ω_{max}	16000	rpm
Motor to wheel transmission ratio	$\tau_{drivetrain}$	3.36	-

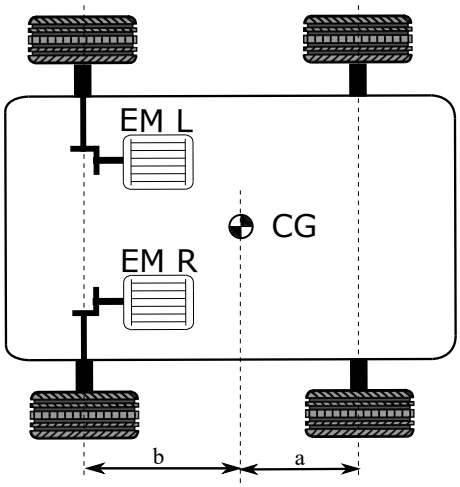

Fig. 1. Vehicle powertrain layout.

included. The tires are modeled with Pacejka's Magic formula with combined slip model which includes first order relaxation length dynamics as well [8]. The vehicle characteristics are chosen similar to that of a standard sedan car (Table I). The inertia of the electric motors are neglected since they are very small when compared to the inertia of the wheels.

The vehicle architecture can be seen in Fig. 1. The electric motors are modeled with the help of torque-speed maps and the effect due to the electrical dynamics are neglected since the vehicle dynamics is much slower that the internal dynamics of the motors. The power consumption is obtained with the help of efficiency maps. Regenerative braking is applied on the rear wheels with the help of the electric motors which provides with the recuperation of braking energy. The braking split ratio is kept fixed at 60-40 (front-rear). It may be argued that most of the braking should be done with the electric motors and the rest could be done with the front friction brakes. However, since the objective of this work is to improve the performance of the vehicle, braking split ratio is kept identical to that of the hydraulic friction braking system to avoid loss of stability [9].

III. TORQUE VECTORING

A. Principles of Torque Vectoring

Vehicle maneuverability is limited by the forces the tires can generate at a given instant of time. These limits can be represented by a friction ellipse which represents a boundary for the maximum forces in the lateral and longitudinal direction [10]. The maximum performance can be extracted from a vehicle when all four tires are working on the boundary of this friction ellipse and thus, they are generating the maximum amount of available force. Racing drivers have a special ability to sense these limits and they are able to make the tires work always close to this region. However, it is not always possible to extract the full potential of every tire. For instance, when a vehicle is cornering there is transfer of vertical load from the inner wheel to the outer wheel. This means that to stay within the limit of the friction ellipse, the inner wheel should generate smaller amount of forces compared to the outer wheel. Conventional differentials impose almost the same amount of driving torque on the left and the right wheels. Thus, the maximum total driving moment is limited by the grip level of the inner wheel. TV allows to exploit the available extra grip in the outer wheel by transmitting more torque to the outer wheel and less torque to the inner wheel so that both tires can work well within their limits and still generate the same amount of driving moment [6]. This can be visualized in Fig. 2. The figure shows left and right tires of a given axle (denoted by L, R respectively). The vehicle is assumed to be cornering in the left direction which introduces higher load on the right wheel. As a result the friction ellipse of the right tire, which denotes its maximum force limit is larger than the left tire. It can be noticed that due to TV, the axle is able to generate higher lateral forces for the same amount of longitudinal axle force.

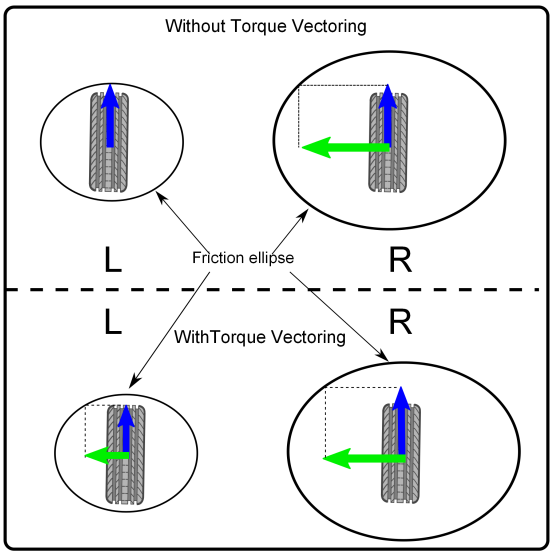

Fig. 2. Increase in lateral force while turning left by the use of torque vectoring (blue - F_x, green - F_y).

A second effect as a result of TV is that it improves the cornering dynamic response of a vehicle. The yaw moment which is generated as a result of torque vectoring can also act as a way to control the tire sideslip angle of the rear tires. Thus with torque vectoring the rear tires are able to generate higher

forces more quickly than the rear tires of a passive vehicle. It is however important to remember that the yaw moment should not increase the rear tire sideslip angle beyond the point of the saturation level of the tires. Such effects can be controlled with an outer layer control or envelope controller which makes sure that the sideslip angle doesn't increase beyond a certain threshold value [11].

B. Control algorithm for Torque Vectoring

Since the vehicle in this study is understeering by nature under steady state conditions, the slip angle of the front tire is always higher than the slip angle of the rear tire. TV to the outer wheel can be used to generate a yaw moment. This leads to an increase in the rear tire sideslip angle and thus, the difference between front and rear tire sideslip angles reduces. If controlled in a proper manner, it is possible to make the front and rear tires go into saturation together (if they do at limit conditions). This will lead to maximum possible lateral force. Thus the desired torque vectoring moment should be the one which keeps the difference between the front and the rear tire sideslip angles to zero.

In this context, the implemented TV control architecture is illustrated in Fig. 3. The reference slip angle difference is set to zero so that the vehicle achieves a neutral steer characteristics. The actual difference between the front and rear tire sideslip angles are computed in the tire slip calculation block as indicated in [12]. This block receives sensor measurements such as yaw rate, vehicle longitudinal velocity, roll angle and the steering angle from the vehicle block. For the slip angle computation, the vehicle can be represented by a bicycle model as seen in Fig. 4. Using kinematics, the slip angles of the front and rear tires denoted by α_f, α_r can be written as

$$\alpha_f = \beta + \frac{ar}{u} - \delta, \tag{1}$$

$$\alpha_r = \beta - \frac{br}{u} - \delta_{roll}, \tag{2}$$

where β is the sideslip angle, r is the yaw rate, u is the vehicle velocity along the longitudinal axis, δ is the input steer by the driver at the front tire and δ_{roll} is the steer at the rear tire due to roll. From (1) and (2), the difference between the front and rear tire slip angles can be written as

$$\alpha_f - \alpha_r = \frac{(a+b)r}{u} - \delta + \delta_{roll}. \tag{3}$$

The yaw rate and roll angle signals are obtained from a three axis gyroscope placed at the CG of the vehicle. The front tire steer angle is obtained by measuring the steering angle at the steering wheel and then using a lookup table which models the steering system. It is interesting to notice that the sideslip angle gets eliminated from the picture in (3). This is advantageous since sideslip measurement or robust sideslip estimation is generally not possible in normal production vehicles. A simplified model for obtaining the roll steer is implemented as

$$\delta_{roll} = \mathrm{K}_{\mathrm{rollsteer}}\phi, \tag{4}$$

where $\mathrm{K}_{\mathrm{rollsteer}}$ is the roll steer constant and ϕ is the roll angle. Fig. 5 presents the validation of the roll steer model.

The high level controller consists of a PD controller. The input to the PD controller is the error in the desired value of the difference between the front and rear tire sideslip angles. The output of the controller is the TV torque contribution, which is represented by T_{TV} and it can be written as

$$T_{\mathrm{TV}} = \mathrm{K_p}(\alpha_f - \alpha_r) + \mathrm{K_d}\frac{d(\alpha_f - \alpha_r)}{dt}, \tag{5}$$

where $\mathrm{K_p}$ and $\mathrm{K_d}$ are the proportional and derivative feedback constants respectively. In the following simulations, $\mathrm{K_p}$ is set to -20000/$\tau_{\mathrm{drivetrain}}$ and $\mathrm{K_d}$ is set to $-\mathrm{K_p}/100$. A saturation block is added to the output of the PD controller which saturates its value to the maximum rated torque of the electric motors as seen in Table I.

The low level controller is responsible for the allocation of torque to the individual rear electric motors and to also activate rear wheel friction brakes when necessary. The layout of the low level controller can be visualized in Fig. 6. The dotted rectangle encloses the two components of the low level controller. The torque allocation block is responsible for dividing the requested driving torque T_{req} equally between the left and right motors. It is assumed that the electric motors work as ideal reversible machines and produce equal amount of torque in opposite direction during regenerative braking mode. If the braking torque demand is higher than the braking capability of the electric motors, the low level controller activates the rear wheel friction brakes to fill in the extra braking torque demand on each wheel. The torque allocation is represented as follows,

$$T_{EML,R} = \begin{cases} \frac{T_{req}}{2} & \text{if } T_{req} > -2T_{max(\omega)} \quad (6) \\ -T_{max(\omega)} & \text{if } T_{req} \leq -2T_{max}(\omega) \quad (7) \end{cases}$$

$$T_{FB} = \begin{cases} 0 & \text{if } T_{req} > -2T_{max(\omega)} \quad (8) \\ \frac{T_{req}}{2} + T_{max(\omega)} & \text{if } T_{req} \leq -2T_{max}(\omega), \quad (9) \end{cases}$$

where T_{FB} denotes the rear wheel friction brake demand. The braking torque due to the friction brakes on the left and the right wheels are considered to be of the same magnitude due to the absence of an active hydraulic braking circuit present in the baseline passive vehicle. The second block in the low level controller is responsible for the addition of the torque required for generating the requested TV moment. It takes the torque outputs of the torque allocation block as input and adds the contribution from high level TV controller denoted by T_{TV}. The block is designed such that the sum of the torques acting on the left and the right wheel always become equal to the traction/braking torque demand. Thus when the sum of the torque contributions due to driver torque demand and TV controller demand on a motor is larger than the maximum motor torque, the torque due to torque vectoring is reduced so that the net torque request on each motor is always within

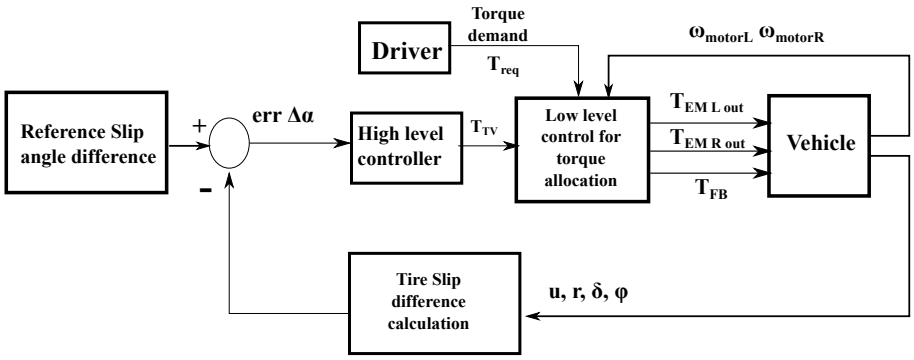

Fig. 3. Overview of the control architecture.

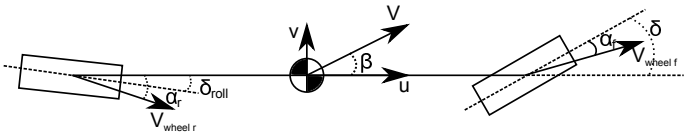

Fig. 4. Bicycle model representation of the vehicle.

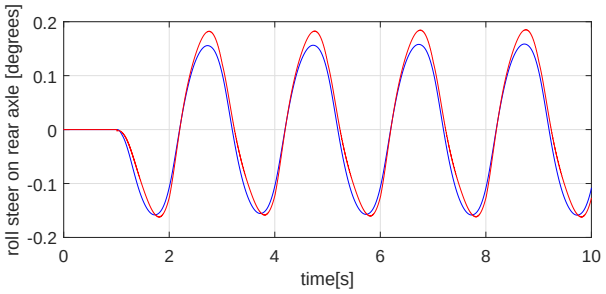

Fig. 5. Validation of the roll steer model with a sine steer maneuver at 100kph and steer amplitude of 30 degrees on the steering wheel (blue- equation (4), red - measured from vehicle).

the maximum torque limit of the motor. The motor torque computation for this block is expressed as follows:

$$T_{lim} = min(T_{max(\omega)} - |T_{EML}|, T_{max(\omega)} - |T_{EMR}|), \quad (10)$$

$$\Delta T = min(T_{lim}, |T_{\mathrm{TV}}|)sign(T_{\mathrm{TV}}), \quad (11)$$

$$T_{EMLout} = T_{EML} + \Delta T, \quad (12)$$

$$T_{EMRout} = T_{EMR} - \Delta T, \quad (13)$$

where T_{lim} defines the maximum limit of torque available for TV, ΔT represents the torque added on the left wheel due to TV, T_{EMLout}, T_{EMRout} represent the actual amount of torque applied on the left and right rear wheel respectively.

IV. Results

Simulations are carried out with the vehicle model described in section II. Both open and closed loop maneuvers are carried out. An expert driver model is chosen to control the vehicle. The motivation behind this choice is to be able to extract the maximum possible performance of a vehicle in closed loop maneuver without suffering from the need of using the intervention of safety systems like Anti-lock Braking systems

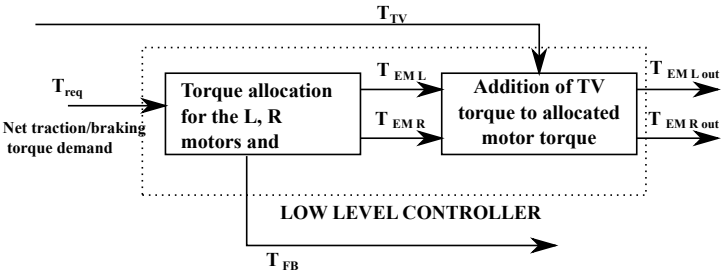

Fig. 6. Schematic of the low level controller.

and Traction Control Systems. The driver commands are optimized offline so as to obtain the best possible performance with respect to lap-times.

A. Ramp steer at constant velocity

An open loop ramp signal is applied to the steering angle while keeping the velocity of the vehicle constant with the help of cruise control. The test is carried out at 72km/h on a dry road with peak friction of coefficient(μ) equal to 1 with a steering angle ramp of 5.729 deg/s (0.1rad/s). When TV is switched on, there is an improvement of 10.15% in the understeer gradient and an increment of about 3% in the maximum lateral acceleration. Fig. 7 demonstrates the performance improvements of the active vehicle mentioned above. It is also observed that higher yaw rate is generated in the case with TV on. It can be seen that after 15 seconds, when the tires reach their saturation limit, the vehicle with TV on remains stable as there is not exponential increase in the yaw rate. However, in the vehicle with TV off, the yaw rate increases drastically and the vehicle spins off.

B. Flying lap around Hockenheim

Simulations are carried for flying laps on the Hockenheim circuit in order to understand the performance improvement of the vehicle due to TV. The driver controller gives inputs to the steering wheel such that the vehicle follows the fastest racing line around the track. This racing line is available beforehand as track data and acts as reference input for the controller. An offline optimization allows to determine the fastest velocity profile at which the car can go around the track.

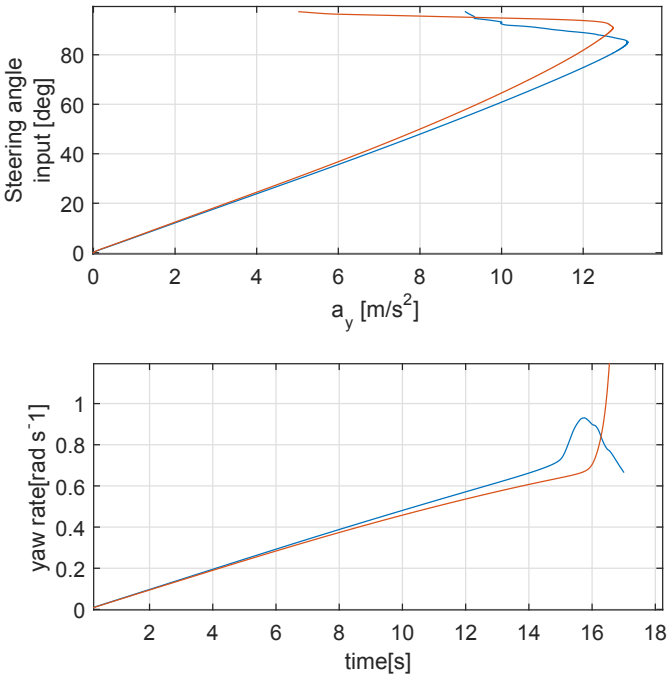

Fig. 7. Improvement in maximum lateral acceleration and understeering gradient with Torque vectoring (red - without TV, blue -with TV).

This information is stored as a speed vs. distance map. The driver controller the feeds the throttle and brake demand so that the vehicle speed profile matches this speed vs. distance map. Fig. 8 shows the speed profile during one flying lap around the track for the vehicle with TV on and off. It can be observed that the vehicle can go around the track faster when TV is switched on. The passive vehicle takes about 76.2 seconds to complete one lap. The lap time reduces by around 2.1 sec when TV is switched on. Most of this time is saved while going around corners at higher speed. Such behavior can be seen at the local minima of the speed vs. time plot shown in Fig. 8. The regions around these local minima give the velocity of the vehicle while it goes in and subsequently out of the various corners of the track. It can be clearly seen that on each and every corner the vehicle with TV on has a higher velocity throughout the cornering maneuver. As a result of the higher speeds through one corner after another, the velocity profile of the passive vehicle starts lagging in time when compared to the velocity profile of the active vehicle. TV allows generation of higher lateral acceleration values which in turn leads to higher velocities around corners. This gain can be also seen in Fig. 9 as TV leads to enlargement of the a_x vs. a_y plot. The enlargement in the a_x vs. a_y plot can be most prominently noticed in the area where a_x lies between 0 m/s and -7 m/s and a_y lies between 5 m/s and 15 m/s. Since the track has mostly left hand turns and by convention the lateral acceleration is positive in the left direction, it can be understood that the enlargement of the a_x vs. a_y plot takes place mostly when the vehicle is braking into a turn. Similar gains can be also seen in the zone where a_x is positive and

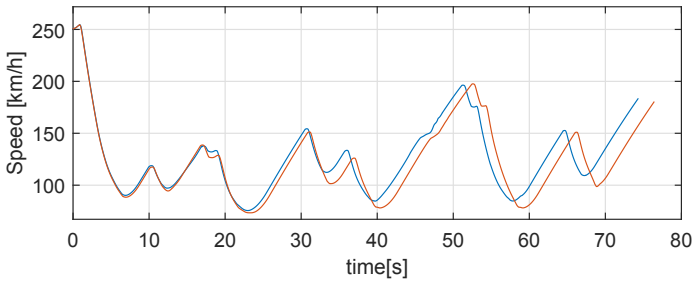

Fig. 8. Fastest velocity profile for a flying lap around Hockenheim (red - without TV, blue -with TV).

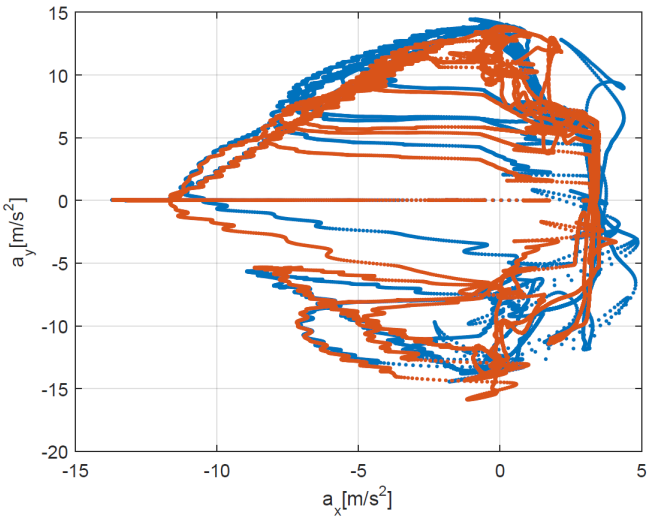

Fig. 9. $a_x - a_y$ plot (red - without TV, blue -with TV).

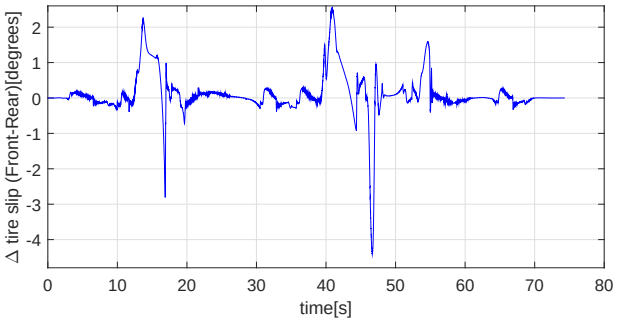

Fig. 10. Difference between the average (L, R) front and rear tire sideslip angles for a flying lap around Hockenheim with TV on.

a_y lies between 5 m/s and 15 m/s, which indicates that even when the vehicle is exiting the corner, it is able to generate higher lateral forces. Moreover, the tire slip angles of the front and rear tires are close to each other when TV is switched on. The maximum difference between the slip angles is around 5 degrees and the average value staying very close to zero as seen in Fig. 10. Without TV, the difference between the front and rear tire slip angle increases up to 12 degrees as seen in Fig. 11.

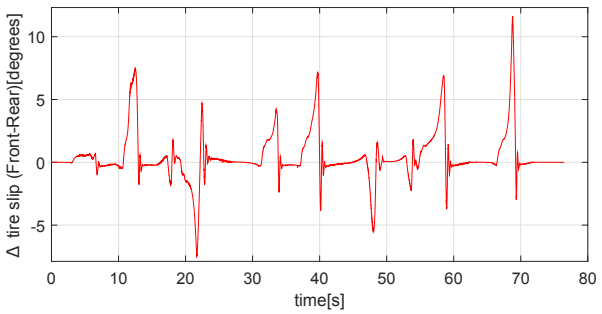

Fig. 11. Difference between the average (L, R) front and rear tire sideslip angles for a flying lap around Hockenheim with TV off.

C. Double lane change maneuver

A double lane change maneuver at 90 km/h was simulated as seen in Fig. 12. It is can be noticed that the sum of the two motor torques in the case with TV on is equal to the net motor torque output in the case with TV off. Also, when TV is switched on, the yaw rate response becomes faster due to the generation of yawing moment by the TV system. Similarly it can be seen that the steering input by the driver in the case with TV on is smaller in magnitude as compared to the case with TV off. This indicates that the driver requires less effort to execute the same maneuver, which is advantageous in emergency situations. In addition, it is also noticed that the driver steering input is smoother in the case of TV, while the driver steering input looks very nervous in the case without TV.

V. Conclusions

A feedback based TV controller for a rear wheel drive electric vehicle was presented in this article. Numerical simulations with a multi-body vehicle model indicate that the controller is able to improve handling performance. Results from ramp steer maneuver show that there is an improvement of about 10% in the understeer gradient of the vehicle. Moreover, the controlled vehicle is able to avoid spinning once it exceeds the maximum tire limits while passive vehicle spins out in similar conditions. Flying lap simulations on a race track demonstrate that the controlled vehicle is able to extract higher tire forces and as a result it is able to go faster around the track. Double lane change simulations indicate that TV improves the vehicle response in emergency situations making it easier for the driver to execute the maneuver.

Future scope of work could be adding an additional layer of envelope control to take care of vehicle safety when driven by novice drivers as demonstrated in [11], [13].

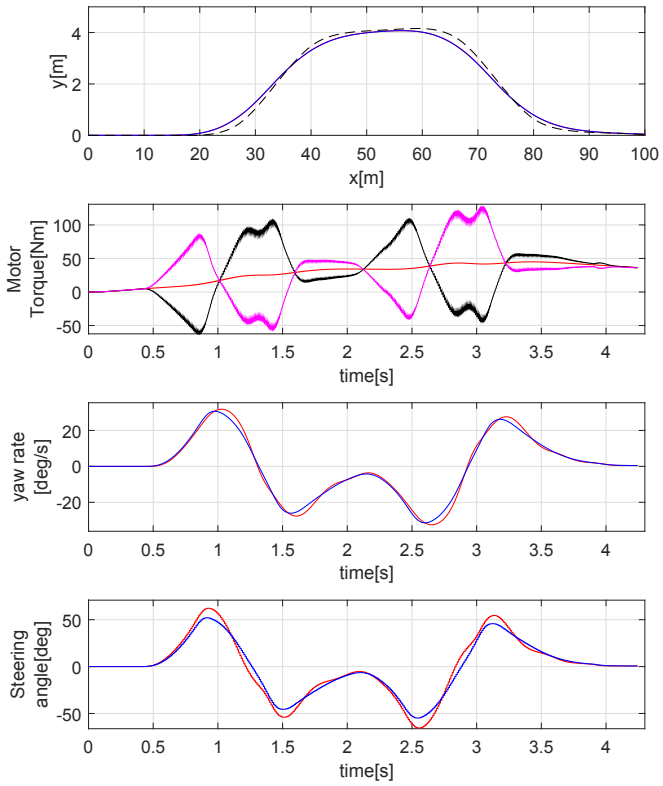

Fig. 12. Double lane change maneuver at 90 km/h; black dashed curve - desired path; red- TV off; blue- TV on; black - left motor torque; magenta- right motor torque.

References

[1] Y. Shibahata, K. Shimada, and T. Tomari, "Improvement of vehicle maneuverability by direct yaw moment control," *Vehicle System Dynamics*, vol. 22, no. 5-6, pp. 465–481, 1993.

[2] M. Abe, "Vehicle dynamics and control for improving handling and active safety: from four-wheel steering to direct yaw moment control," *Proceedings of the Institution of Mechanical Engineers, Part K: Journal of Multi-body Dynamics*, vol. 213, no. 2, pp. 87–101, 1999.

[3] L. De Novellis, A. Sorniotti, and P. Gruber, "Wheel torque distribution criteria for electric vehicles with torque-vectoring differentials," *Vehicular Technology, IEEE Transactions on*, vol. 63, no. 4, pp. 1593–1602, 2014.

[4] L. De Novellis, A. Sorniotti, P. Gruber, L. Shead, V. Ivanov, and K. Hoepping, "Torque vectoring for electric vehicles with individually controlled motors: state-of-the-art and future developments," in *26th Electric Vehicle Symposium 2012*, 2012.

[5] F. Braghin, E. Sabbioni, G. Sironi, and M. Vignati, "A feedback control strategy for torque-vectoring of iwm vehicles," in *ASME 2014 International Design Engineering Technical Conferences and Computers and Information in Engineering Conference*. American Society of Mechanical Engineers, 2014, pp. V003T01A004–V003T01A004.

[6] K. Sawase and Y. Ushiroda, "Improvement of vehicle dynamics by right-and-left torque vectoring system in various drivetrains," *Mitsubishi Motors Technical Review*, vol. 20, p. 14, 2008.

[7] T. D. Gillespie, "Fundamentals of vehicle dynamics," SAE Technical Paper, Tech. Rep., 1992.

[8] H. Pacejka, *Tire and vehicle dynamics*. Elsevier, 2005.

[9] M. Hancock, "Impact of regenerative braking on vehicle stability," in *Hybrid Vehicle Conference, IET The Institution of Engineering and Technology, 2006*. IET, 2006, pp. 173–184.

[10] G. Genta and L. Morello, "The automotive chassis," 2009.

[11] T. Chung and K. Yi, "Design and evaluation of side slip angle-based vehicle stability control scheme on a virtual test track," *Control Systems Technology, IEEE Transactions on*, vol. 14, no. 2, pp. 224–234, 2006.

[12] L. Segel, "Theoretical prediction and experimental substantiation of the response of the automobile to steering control," *Proceedings of the Institution of Mechanical Engineers: Automobile Division*, vol. 10, no. 1, pp. 310–330, 1956.

[13] C. G. Bobier and J. C. Gerdes, "Staying within the nullcline boundary for vehicle envelope control using a sliding surface," *Vehicle System Dynamics*, vol. 51, no. 2, pp. 199–217, 2013.